Computational Materials Science 82 (2014) 197–201

Contents lists available at ScienceDirect

Computational Materials Science

journal homepage: www.elsevier.com/locate/commatsci

Hydrogen fluoride on the pristine, Al and Si doped BC_2N nanotubes: A computational study

Ali Ahmadi Peyghan [a], Maziar Noei [b,*]

[a] Central Tehran Branch, Islamic Azad University, Tehran, Iran
[b] Department of Chemistry, Mahshahr Branch, Islamic Azad University, Mahshahr, Iran

ARTICLE INFO

Article history:
Received 31 May 2013
Received in revised form 23 September 2013
Accepted 25 September 2013

Keywords:
Inorganic nanotube
B3LYP-D
Sensor
DFT

ABSTRACT

We investigated the electronic sensitivity of a BC_2N nanotube to a HF molecule by density functional calculations at B3LYP (augmented with an empirical dispersion term) level of theory. It was found that the HF molecule prefers to be weakly adsorbed on the tube with the adsorption energy of 23.1 kcal/mol and without significant effect on its electronic properties. Al and Si dopings into the wall of the tube increase the reactivity of the tube toward the HF molecule, so that calculated adsorption energies are about 92.8 and 73.0 kcal/mol, respectively. Contrary to the Al doping, the Si doping significantly enhances the electronic sensitivity of the tube to the HF molecule. We believe that Si-doped BC_2N nanotube can convert the presence of HF molecules to an electrical signal which will be useful in the detection process.

1. Introduction

Carbon exists in several forms in nature and one of the carbon allotropes is carbon nanotubes (CNTs) with cylindrical form that discovered in 1991 by Iijima [1]. CNTs have novel properties, making them potentially useful in many applications in nanotechnology, nanoelectronics, optics, and other fields of materials science [2,3]. Nanotube-based electronic devices, such as diodes, transistors, or field emitters, rely on modifications of the electronic properties of CNTs caused by mechanical deformations, doping or topological defects. Substituting CNTs with other elements like B, N can tune their electronic properties efficiently and lead to novel applications [4]. The BC_2N stoichiometry is believed to be one of the most stable forms of the ternary BCN layers and nanotubes [5]. Bariele et al. have investigated theoretically stability and hydrogen adsorption properties of BC_2NNT [6,7]. Considerable experimental and theoretical efforts have been devoted to the synthesis of BC_2NNTs, and they have been successfully obtained by electrical pyrolysis, laser ablation, hot-filament chemical vapor deposition, and the template route [8–11].

Nowadays, it is essential to be able to quickly analyze and control the surrounding atmosphere in order to prevent the possible risks of pollution. With this in mind, many groups decided to work on the development of gas sensors for measuring toxic chemical compounds. Nanotubes exhibit potential applications in this field because of their unique properties such as high surface to volume ratio. Basically, it is expected that the adsorption of gas molecules on the sensors is stable and conductivity changes should be observable. However, most of gases are found physisorbed on suspended intrinsic nanotubes [12–14]. On the contrary, the dopants and defects in nanotubes can strongly enhance the adsorption of molecules [15,16], indicating that doped atoms and defects play important roles in their applications. Peyghan et al. [17] have investigated adsorption mechanisms of hydrogen cyanide on modified BC_2NNT, including aluminum doping and double anti-site defect using density functional theory (DFT). It was found that the BC_2NNT with double anti-site defect is more sensitive than perfect tube for detecting hydrogen cyanide.

In the present work, within the DFT framework, the interaction of hydrogen fluoride (HF) with BC_2NNTs will be investigated based on analyses of structure, energies, electronic properties, etc. Among the dangerous chemical compounds for both human and the environment, one can distinguish HF. HF is involved in a very specific chemical process and it can be released in the atmosphere [18]. In this case, it is essential to be able to quickly analyze this molecule in order to prevent the possible risks of pollution. It is also a degradation product from fire suppression systems that use Halon 1301 (bromotrifluoromethane) and Halon 1211 (bromochlorodifluoromethane) as fire suppression agents [18]. We are interested in whether there is a possibility of BC_2NNTs serving as a chemical sensor to HF molecule, and if not, can we find a method to improve the sensitivity of BC_2NNTs to HF?

* Corresponding author.
E-mail address: noeimaziar@gmail.com (M. Noei).

0927-0256/$ - see front matter © 2013 Elsevier B.V. All rights reserved.
http://dx.doi.org/10.1016/j.commatsci.2013.09.058

2. Computational methods

We selected a (8,0) BC_2NNT consisted of 32 B, 32 N and 64 C atoms, in which the end atoms have been saturated with hydrogen atoms to reduce the boundary effects. Geometry optimizations, energy calculations, natural bond analysis (NBO) and density of states (DOS) analysis have been performed on BC_2NNT and different HF/BC_2NNT complexes using B3LYP functional augmented with an empirical dispersion term (B3LYP-D) with 6-31G (d) basis set as implemented in GAMESS suite of program [19]. GaussSum program has been used to obtain the DOS results [20]. The B3LYP has been demonstrated to be a reliable and commonly used functional in the study of different nanostructures [21–25]. We have defined the adsorption energy in the way as:

$$E_{ad} = E(HF) + E(BC_2NNT) - E(HF/BC_2NNT) + E_{BSSE} \quad (1)$$

where E (HF/BC_2NNT) corresponds to the energy of the BC_2NNT, in which HF has been adsorbed on the surface, E (BC_2NNT) is the energy of the isolated tube, E (HF) is the energy of a single HF molecule, and E_{BSSE} is the energy of the basis set superposition error (Tables 1 and 2).

3. Results and discussion

3.1. Pristine BC_2NNT

In Fig. 1a, we have shown the optimized structure of BC_2NNT, where four types of bonds, namely B–N, B–C_I, N–C_{II} and C_I–C_{II}, can be identified, with corresponding lengths of 1.46, 1.52, 1.44 and 1.36 Å, respectively. C_I is a carbon atom that is bonded to two B atoms and one C atom, while C_{II} is bonded to two N atoms and one C atom. Buckling of B–N and C–C bonds was found in the wall of the tube. After optimization, this buckling moves N atoms slightly inward and B atoms outward of the nanotube surface in the B–N bonds. On the other hand, for C–C bonds, the C_I atoms are relaxed outward, while the C_{II} atom is relaxed inward of the nanotube surface. Buckling of atoms from perfect cylindrical model is a solution to minimize the total energy and strain energy.

In order to find the most stable site for HF adsorption on the tube, the HF molecule was initially located on different sites; the hydrogen or flour atom of HF was located on the top of a tube's atom, the center of different hexagonal ring of BC_2NNT and also the bridge site of B–N, B–C_I, N–C_{II} and C_I–C_{II} bonds. To ensure that the most stable configuration is achieved, the initial distance between the molecule and the tube was adjusted several times from 1.0 to 3.0 Å. Without any constrain, full structural relaxation was then performed on each initial configuration. However, only one local minimum structure was obtained after the relaxation process (Fig. 1b). In this configuration, HF molecule was located on the top of B–C_I bond, so that two new bonds, namely F–B and H–CI, with lengths of 2.09 and 2.06 Å were formed, respectively. More detailed information from the simulation of the HF/BC_2NNT systems, including values of E_{ad}, electronic properties and the charge transfer (Q_T) for these configurations is listed in Table 1. The calculated molecular electrostatic plot of HF shows that the exothermic nature of this interaction (E_{ad} = 23.1 kcal/mol) is because of the partial negative charge on the F atom which makes it reactive toward the Lewis acid sites of B atoms. Based on NBO charge analysis, a 0.113e was transferred from the molecule to the nanotube. It is worth saying that other initial configurations re-oriented to this stable configuration.

To investigate the effect of adsorption process on the electronic properties of pristine BC_2NNT, the DOS plots were calculated for the tube and HF/tube complex. As shown by the calculated DOS and the energy gaps (E_g) between the highest occupied molecular orbital (HOMO) and the lowest unoccupied molecular orbital (LUMO) in Fig. 1a and Table 1, the pristine BC_2NNT is found to be a semiconductor with the E_g of 1.95 eV. By referring to Fig. 1b, both conduction and valence levels slightly move to higher energies, so that E_g of the tube slightly decreased to 1.92 eV for HF/BC_2NNT complex because of the charge transfer to the tube. This change in electronic properties is negligible indicating that BC_2NNT is still a semiconductor after HF adsorption. Thus, we conjecture that the electronic properties of pristine BC_2NNT are insensitive to the HF molecule.

3.2. Al-doped BC_2NNT

To overcome the insensitivity of the BC_2NNT to the HF, the adsorbing B atom was replaced by an Al atom. By substituting the B atom using the impurity of Al, the geometric structure of the BC_2NNT is dramatically distorted (Fig. 2a). In the optimized

Table 1
Calculated adsorption energy of a HF (E_{ad}, kcal/mol), energy of basis set superposition error (E_{BSSE}, kcal/mol), HOMO energies (E_{HOMO}), LUMO energies (E_{LUMO}), and HOMO–LUMO energy gap (E_g) for pristine BC_2NNT in eV.

System	E_{ad}	E_{BSSE}	Q_T (e)[a]	E_{HOMO}	E_{LUMO}	E_g	ΔE_g (%)[b]	$D_{H\text{-}F}$ (Å)[c]
BC_2NNT	–	–	–	−5.16	−3.21	1.95	–	–
HF/BC_2NNT	23.1	1.2	0.113	−5.11	−3.19	1.92	1.5	0.98

[a] Q is defined as the average of total NBO charge on the molecule.
[b] The change of HOMO–LUMO gap of BC_2NNT after HF adsorption.
[c] H–F bond distance for adsorbed molecule (the bond for isolated molecule is 0.93 Å).

Table 2
Calculated adsorption energy of HF (E_{ad}, kcal/mol), energy of basis set superposition error (E_{BSSE}, kcal/mol), HOMO energies (E_{HOMO}), LUMO energies (E_{LUMO}), and HOMO-LUMO energy gap (E_g) for doped BC_2NNT in eV.

System	E_{ad}	E_{BSSE}	Q_T (e)[a]	E_{HOMO}	E_{LUMO}	E_g	ΔE_g (%)[b]	$D_{H\text{-}F}$ (Å)[c]
Al-BC_2NNT	–		–	−5.20	−3.25	1.95	–	–
HF/Al-BC_2NNT	92.8	3.3	−0.121	−5.16	−2.45	1.71	12.3	1.23
Si-BC_2NNT	–		–	−5.22	−3.42	1.80	–	–
HF/Si-BC_2NNT	73.0	2.7	0.119	−3.83	−3.21	0.62	65.5	1.47

[a] Q is defined as the average of total NBO charge on the molecule.
[b] The change of HOMO–LUMO gap of doped BC_2NNT after HF adsorption.
[c] H–F bond distance for adsorbed molecule (the bond for isolated molecule is 0.93 Å).

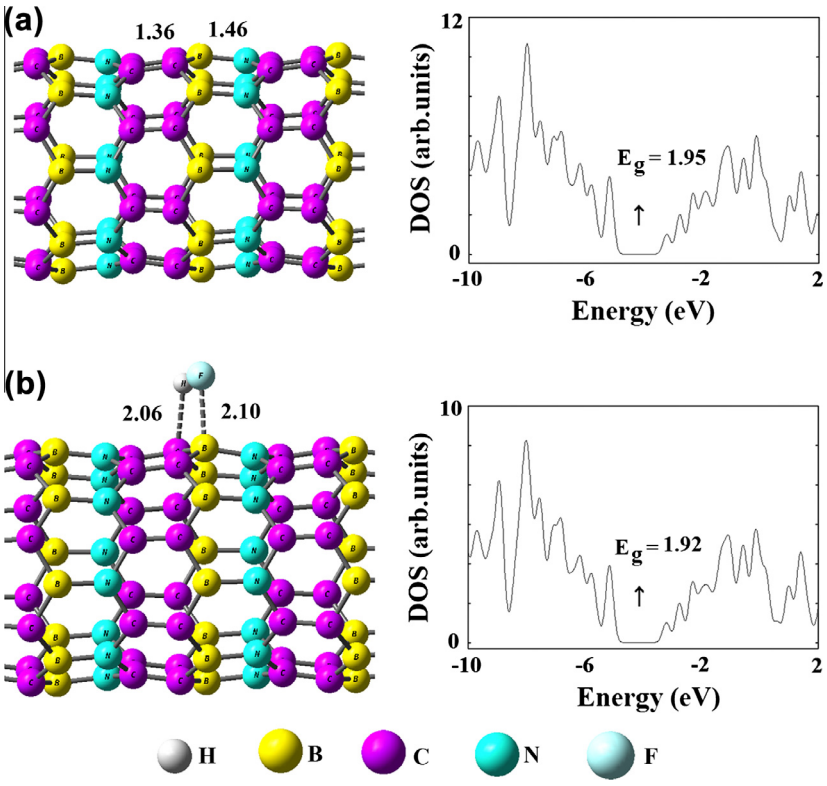

Fig. 1. Optimized structure (partial) of (a) BC_2NNT, (b) HF/BC_2NNT and their density of states (DOS). Distances are in Å.

Al-doped BC_2NNT, the Al atom impurity is projected out of the surface to reduce the stress because of its larger size compared to the B atom. The calculated bond lengths are 1.78 Å for the neighboring Al–N bond in the doped tube which is much longer than the corresponding B–C bonds in the pure tube. Also, the C_l–Al–C_l angle in the doped tube is 109.2° which is smaller than C_l–B–C_l in the pure one (117.1°), which NBO analysis suggests that it can be attributed to the change of doped site hybridization from sp^2 to nearly sp^3. Calculated DOS of Al-doped BC_2NNT is shown in Fig. 2a, indicating that its E_g value is 1.95 eV, which is similar to pristine tube.

Subsequently, we have explored HF adsorption on the Al-doped tube by locating the molecule above the Al atom with different initial orientations including an F or H atom of the molecule which is close to Al. After relax optimization of initial structures, only one final stable structure was obtained which is shown in Fig. 2b. During the optimization, the HF reoriented in such a way that its F atom has got closer to the Al site with E_{ad} of 92.8 kcal/mol. Also, the corresponding interaction distance between the Al atom of doped tube and the HF is about 1.66 Å. Smaller bond length of F. . .Al and larger E_{ad} between the Al-doped BC_2NNT and HF indicate that the doping of Al in the BC_2NNT can improve the reactivity of the sheet toward the molecule. The HF binds to the exposed Al atom which is electron-deficient and can receive electrons from the lone pair orbital of flour. In Table 2, we have summarized the results for E_{ad}, charge transfer, and E_g for HF adsorption on the Al-doped tube. DOS plot of the HF/Al-doped BC_2NNT shows a change, indicating that the electronic properties of the Al-doped tube are sensitive to the HF adsorption compared to pristine tube. By refereeing to Fig. 2b, the E_g value of the doped tube is decreased from 1.95 to 1.71 eV in the adsorbed form.

Previously, Zhu et al. have shown that the E_{ad} of HF adsorbed on the graphene was dramatically increased from 2.3 to 11.3 kcal/mol after Ti doping within the generalized-gradient approximation functional with the Perdew–Burke–Ernzerhof correction [23]. They found that Ti doping can also improve the sensitivity of graphene toward HF, so that E_g of Ti-doped sheet decreases from 0.44 to 0.40 eV (by about 9.1% reduction). Although, based on our calculations, aluminum doping can improve the sensitivity of BC_2NNT to HF adsorption by about 12.3% change in E_g, we still think that it is not a promising way for monitoring the trace concentration of HF using BC_2NNT.

3.3. Si-doped BC_2NNT

Thus, in the next step, we studied the doping of BC_2NNT with other elements. Furthermore, the effects of substituting adsorbing boron atom of the tube by a Si atom on the geometrical structure, electronic properties of the tube, and also on the adsorption behaviors were investigated. Also, we have observed that the silicon atom projects out of the sheet and creates local deformation because of larger covalent radius of silicon atom (1.11 Å) in comparison with boron atom (0.90 Å). The deformation at silicon site shows that both (Si–C_l) bonds are of the same length (1.83 Å) and Si–N bond (1.76 Å) is larger than B–C_l and Bi–N bonds (Fig. 3a). The bond angles between C_l–Si–C_l and C_l–Si–N bonds are 99.3° and 101.1°, respectively, which indicate the tetrahedral structure of bonding that prefers sp^3 hybridization. This structural deformation results in a significant change in properties such as E_{ad}, E_g and charge transfer. Baierle et al. results have shown that the Si impurity has lower formation energy for the BC_2NNT as compared with Si-doped CNTs and BNNTs [26].

Mulliken population analysis shows that silicon atom acquires positive charge with the magnitude of 0.514*e* compared to 0.231*e* of boron atom in pristine BC_2NNT. This reveals that the charge is transferred from the silicon atom to the vicinal carbon and nitrogen atoms. Thus, the dopant site (silicon atom) acts as an affinity center for the adsorption of HF molecule. We have performed calculations to predict the interaction of HF with Si-doped tube and found the most stable configuration. As shown in Fig. 3b, the molecule binds to the silicon and nitrogen atoms by forming

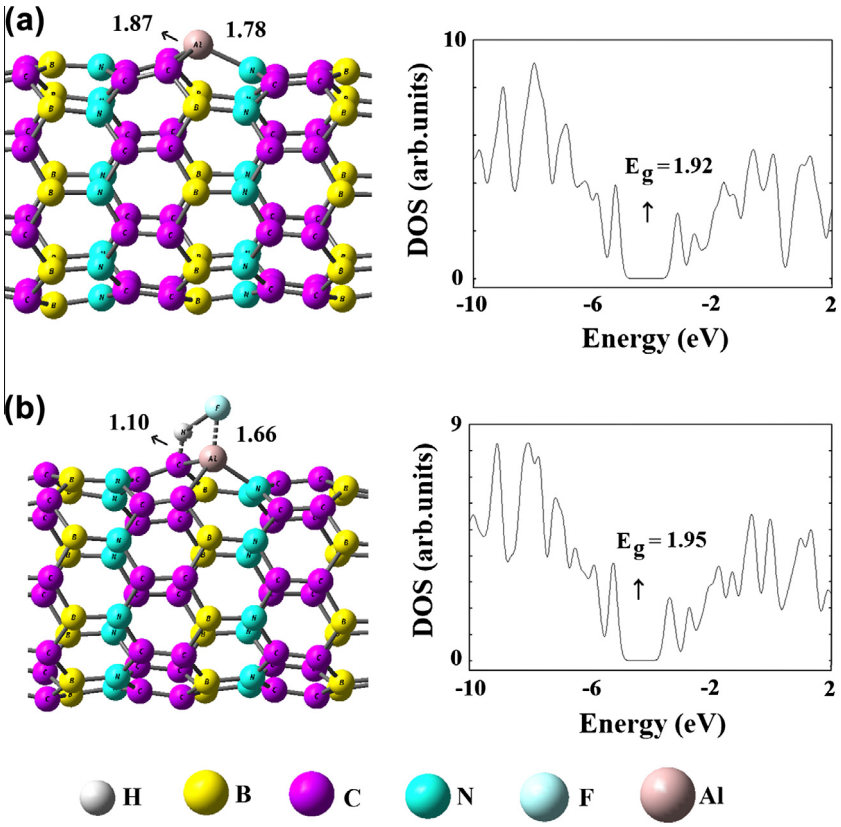

Fig. 2. Optimized structure (partial) of (a) Al-doped BC_2NNT, (b) HF/Al-doped BC_2NNT and their density of states (DOS). Distances are in Å.

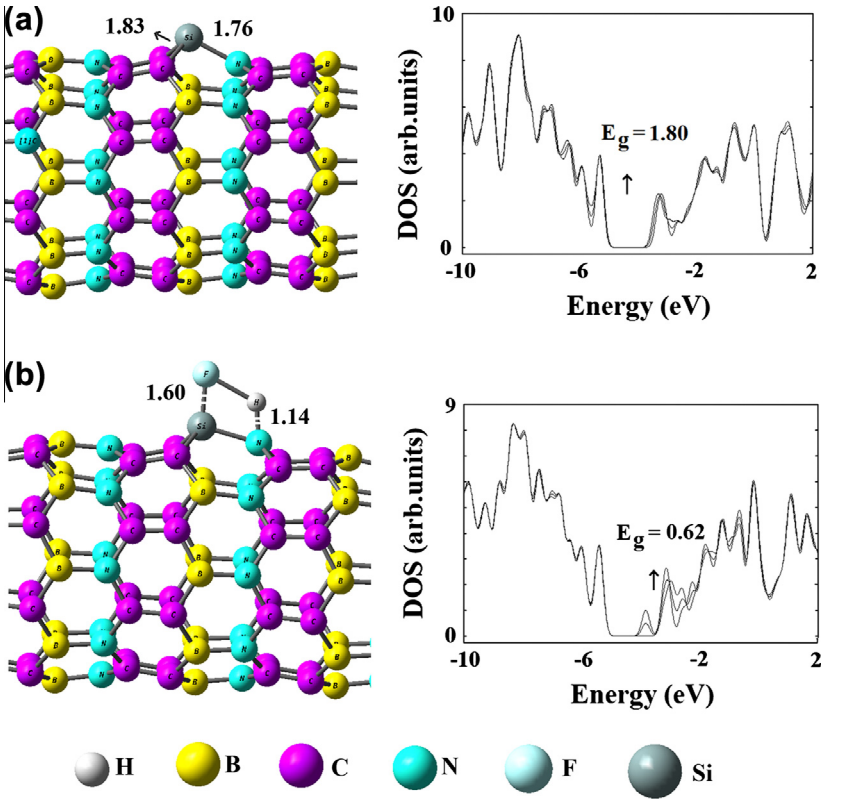

Fig. 3. Optimized structure (partial) of (a) Si-doped BC_2NNT, (b) HF/Si-doped BC_2NNT and their density of states (DOS). Distances are in Å. The studied systems are open shell with an unpaired electron. Red, green and blue curves designate alpha, beta and total DOS spectrums, respectively. (For interpretation of the references to colour in this figure legend, the reader is referred to the web version of this article.)

two bonds of Si–F and N–H with lengths of 1.60 and 1.14 Å, respectively, and corresponding E_{ad} of 73.0 kcal/mol. The larger value of E_{ad} indicates that the interaction of HF molecule with Si-doped BC_2NNT is enhanced in comparison with the pure tube.

To better understand the effects of HF adsorption on electrical conductivity, the DOS plots of Si-doped BC_2NNT with and without the adsorption is calculated. Calculated DOS of Si-doped tube is shown in Fig. 3a, indicating that its E_g value is 1.80 eV compared to the pristine BC_2NNT. However, the Si-doping forms a donor-like state, revealing that doping semiconducting BC_2NNT with Si atom will create *n*-type semiconductor, resulting in an increased conductivity. It should be noted that an impurity peak appears at −3.83 eV in DOS of HF/Si-doped tube, thereby reducing the E_g of BC_2NNT from 1.80 to 0.62 eV (Fig. 3b). Appearance of this peak indicates that after adsorbing the HF molecule, the Si-doped tube becomes more semiconductor-like, with a drop in the DOS near the Fermi level, and thus a significant increase in conductance is expected compared to the non-adsorbed sheet. The phenomenon can be explained by the following relation [27]:

$$\sigma \propto \exp\left(\frac{-E_g}{2kT}\right). \quad (2)$$

where σ is the conductance and k is the Boltzmann's constant. According to the equation, smaller E_g values lead to the higher conductance at a given temperature. The considerable change of about 65.5% (Table 2) in the E_g value demonstrates the high sensitivity of the electronic properties of Si-doped tube to the HF. By detecting the conductivity change of the Si-doped BC_2NNT system before and after the adsorption of HF, the presence of this toxic molecule can be detected sensitively and therefore could be potentially used in HF sensors.

4. Conclusion

The adsorption of a HF molecule on the pure, Al- and Si-doped BC_2NNTs was investigated using DFT calculations. It is found that HF molecule is adsorbed on the boron atom of pristine nanotube from its F head with E_{ad} of 23.1 kcal/mol. The electronic properties of the pristine BC_2NNT induce a very limited change after the adsorption of HF molecule. However, the HF molecule shows strong interactions with the Al- and Si-doped tubes. The larger adsorption energies and charge transfers of HF on the modified BC_2NNTs are expected to induce significant changes in the electrical conductivity of the tube, especially in the case of Si-doped one. The results may help to seek appropriate chemical modification methods to widen the application fields of the BC_2NNT.

References

[1] S. Iijima, Nature 354 (1991) 56–58.
[2] A. Montazeri, M. Sadeghi, R. Naghdabadi, H. Rafii-Tabar, Comput. Mater. Sci. 49 (2010) 544–551.
[3] A. Morka, B. Jackowska, Comput. Mater. Sci. 50 (2011) 1244–1249.
[4] L.S. Panchakarla, A. Govindaraj, C.N.R. Rao, Inorg. Chim. Acta 363 (2010) 4163–4174.
[5] X. Blase, J.C. Charlier, A. De Vita, R. Car, Appl. Phys. Lett. 70 (1997) 197–199.
[6] J. Rossato, R.J. Baierle, W. Orellana, Phys. Rev. B 75 (2007) 235401–235407.
[7] J. Rossato, R.J. Baierle, T.M. Schmidt, A. Fazzio, Phys. Rev. B 77 (2008) 035129–035134.
[8] R. Sen, B.C. Satishkumar, A. Govindaraj, K.R. Harikumar, R. Gargi, J.P. Zhang, A.K. Cheetham, C.N.R. Rao, Chem. Phys. Lett. 287 (1998) 671–676.
[9] Ph. Redlich, J. Loeffler, P.M. Ajayan, J. Bill, F. Aldinger, M. Rühle, Chem. Phys. Lett. 260 (1996) 465–470.
[10] X.D. Bai, J.D. Guo, J. Yu, E.G. Wang, J. Yuan, W.Z. Zhou, Appl. Phys. Lett. 76 (2000) 2624–2626.
[11] M.T. Baei, A.A. Peyghan, Z. Bagheri, Solid State Commun. 159 (2013) 8–12.
[12] J. Dai, P. Giannozzi, J. Yuan, Surf. Sci. 603 (2009) 3234–3238.
[13] O. Leenaerts, B. Partoens, F.M. Peeters, Phys. Rev. B 77 (2008) 125416–125421.
[14] T.O. Wehling, K.S. Noveselov, S.V. Morozov, E.E. Vdovin, M.I. Katsnelson, A.K. Geim, A.I. Lichtenstein, Nano. Lett. 8 (2008) 173–177.
[15] J. Dai, J. Yuan, P. Giannozzi, Appl. Phys. Lett. 95 (2009) 232105–232107.
[16] I. Carrillo, E. Rangel, L.F. Magaña, Carbon 47 (2009) 2752–2754.
[17] A.A. Peyghan, N.L. Hadipour, Z. Bagheri, J. Phys. Chem. C 117 (2013) 2427–2432.
[18] S.H. Hoke, Anal. Chim. Acta 460 (2002) 219–225.
[19] M.W. Schmidt, K.K. Baldridge, J.A. Boatz, S.T. Elbert, M.S. Gordon, J.H. Jensen, S. Koseki, N. Matsunaga, K.A. Nguyen, S. Su, T.L. Windus, M. Dupuis, J.A. Montgomery, J. Comput. Chem. 14 (1993) 1347–1363.
[20] N. O'Boyle, A. Tenderholt, K. Langner, J. Comput. Chem. 29 (2008) 839–845.
[21] A. Soltani, M.R. Taghartapeh, E. Tazikeh Lemeski, M. Abroudi, H. Mighani, Superlattices Microstruct. 58 (2013) 178–190.
[22] M.A. Abdulsattar, Superlattices Microstruct. 50 (2011) 377–385.
[23] J. Beheshtian, M. Kamfiroozi, Z. Bagheri, A. Ahmadi, Comput. Mater. Sci. 54 (2012) 115–118.
[24] G. Jian-Jun, Y. Ji-Xian, D. Dong, Physica B 403 (2008) 4033–4037.
[25] E.H. Song, Y.F. Zhu, Q. Jiang, Thin Solid Films (2013), http://dx.doi.org/10.1016/j.tsf.2013.02.047.
[26] C.J. Rupp, J. Rossato, R.J. Baierle, J. Chem. Phys. 130 (2009) 114710–114716.
[27] S. Li, Semiconductor Physical Electronics, second ed., Springer, USA, 2006.